ChemComm

FEATURE ARTICLE

View Article Online
View Journal | View Issue

Cite this: *Chem. Commun.*, 2025, **61**, 2878

Recent innovations in *in situ* strategies to prepare metal–organic framework-based mixed matrix membranes

Liying Zhang, *[a] Yuxin He[a] and Yu Fu *[ab]

Mixed matrix membranes (MMMs) composed of metal–organic frameworks (MOFs) and polymer matrixes have garnered significant attention due to their potential to overcome the permeability–selectivity trade-off inherent in polymeric membranes. Nevertheless, the application and industrial production of MOF-based MMMs have been hindered by issues such as poor interfacial compatibility and cumbersome fabrication processes. Recently, *in situ* strategies have emerged as promising approaches for fabricating MOF-based MMMs, offering enhanced interfacial compatibility between MOF fillers and polymers, as well as a simplified construction process. Furthermore, these strategies enable the creation of cross-linked MMMs with significantly improved interfacial compatibility and mechanical properties, which are unattainable through traditional physical mixing methods. This feature article summarizes recent advancements in the *in situ* preparation of MOF-based MMMs, encompassing *in situ* MOF growth, *in situ* polymerization of polymer matrixes, combined *in situ* methods, and *in situ* post-treatment. Our contributions to the field of *in situ* strategies include the innovative design of efficient spray technology and the formation of asymmetric MMMs. These developments pave the way for the realization of high-performance MOF-based MMMs suitable for industrial applications.

Received 11th December 2024,
Accepted 9th January 2025

DOI: 10.1039/d4cc06508e

rsc.li/chemcomm

Introduction

In the field of membrane technology, using polymeric membranes represents an appealing approach for separation processes, attributed to their ease of fabrication, cost-effectiveness, and energy-saving attributes in industrial applications.

[a] *Department of Chemistry, College of Sciences, Northeastern University, Shenyang 110819, P. R. China. E-mail: zhangliying@mail.neu.edu.cn, fuyu@mail.neu.edu.cn*
[b] *School of Chemical and Environmental Engineering, Sichuan University of Science and Engineering, Zigong 643000, China*

Liying Zhang

Liying Zhang received her doctoral degree in Polymer Chemistry and Physics in 2017 from Jilin University. She then joined Prof. Yu Fu and started her research work on metal–organic frameworks at Northeastern University. In 2021–2022, she worked with Prof. Dr Annette Andrieu-Brunsen at Technical University of Darmstadt as a visiting researcher. Her research interests include defect engineering in metal–organic frameworks and metal–organic framework–polymer hybrids.

Yu Fu

Yu Fu earned a PhD in Polymer Chemistry and Physics in 2003 from Jilin University. After gaining postdoctoral experiences at the University of Leuven in Belgium and Queen's University in Canada, he joined Northeastern University to start his research work on the topology, constitutive morphology and assembly behavior at nano–meso–macroscopic scales. His research interests include porous materials, two dimensional thin films, organic polymers, supramolecules and nanoscience, as well as application areas such as sensing, catalysis and energy.

The inherent trade-off between permeability and selectivity in polymeric membranes has prompted extensive research into the development of MMMs, which combine porous fillers with a polymer matrix to enhance both properties.[1–4] The incorporation of porous fillers has been shown to transcend the permeability–selectivity trade-off.[5]

MOFs composed of metal ions and organic ligands stand out as exceptional porous fillers for MMMs due to their uniform and adjustable pore sizes, high porosity, customizable pore chemistry, and versatile compositions and structures.[6–10] Despite significant research endeavours spanning over two decades, the industrial deployment of MOF-based MMMs remains elusive due to several challenges, including particle agglomeration at desired loadings, insufficient operational stability caused by plasticization and physical aging, and limited scalability for practical industrial applications.

To enhance the separation performance of MMMs, a primary strategy focuses on improving the interfacial compatibility between the filler and the polymer.[11,12] This compatibility is crucial for membrane separation, as it effectively mitigates filler agglomeration and defect formation, which can compromise separation efficiency and mechanical stability over long-term testing. In addition, simplified manufacturing processes are highly desirable to facilitate the practical application of MMMs in industrial settings.

Most of the scientific literature studies dealing with the manufacture of MMMs primarily emphasise the physical mixing method.[13] In a conventional process, pre-synthesised MOF crystals are dispersed in a polymer matrix to form a mixed solution, which is then cast or flat scraped onto suitable flat substrates. Once the membrane is dried by solvent evaporation, a MMM is produced. However, this technique is often plagued by structural imperfections due to poor MOF dispersion. These imperfections not only introduce additional non-selective pathways that reduce separation efficiency, but also compromise mechanical robustness during operation. In addition, the physical mixing method requires the prior synthesis of both MOF crystals and polymers, which hinders industrial-scale production due to its cumbersome and time-consuming process.

Recently, the innovative adoption of *in situ* strategies for the preparation of MMMs, characterised by exceptional MOF dispersion, improved compatibility between MOF fillers and polymers, and a streamlined construction process, has been noteworthy.[14–16] These strategies involve *in situ* MOF growth, *in situ* polymerization of the polymer matrix, and *in situ* post-treatment of the membrane aspects that have not yet been systematically summarized. *In situ* approaches facilitate the adaptive synthesis of MOFs or polymers within a confined space, resulting in a more uniform MOF distribution and a high affinity between the MOFs and the polymers, thereby achieving improved interfacial compatibility.[17] By bypassing the separation and drying steps of MOFs and polymers, *in situ* strategies offer a simpler fabrication process conducive to industrial production, while effectively preventing MOF agglomeration at high loadings.[18]

Notably, *in situ* strategies are also applicable to cross-linking within MMMs, including cross-linking of polymer matrixes and cross-linking between MOFs and polymers, which can significantly enhance interfacial compatibility and mechanical properties.[19,20] This cross-linked structure within MMMs is inaccessible through traditional physical mixing methods.[21] Taking advantage of *in situ* strategies, our research group has developed a novel spraying technique known as "soft spray" for *in situ* MOF growth and simultaneous formation of MOF fillers and a polymer matrix, which offers potential for rapid and large-scale industrial production of MMMs at room temperature.[22–24] Moreover, asymmetric MMMs with high potential for practical applications, and two dimensional (2D) MOF-based MMMs have also been prepared through *in situ* strategies based on the studies of our group.[25–29] Additionally, *in situ* post-treatment of MMMs is emerging as a method to improve interfacial compatibility by removing unavoidable defects or introducing additional interactions between MOFs and polymers.[30,31]

This feature article is divided into four different categories, each focusing on different *in situ* preparation mechanisms of MMMs: *in situ* MOF growth, *in situ* polymerization of polymer matrixes, combined *in situ* methods, and *in situ* post-treatment. It highlights the innovative *in situ* strategies employed to fabricate MOF-based MMMs, providing valuable background information and showcasing recent achievements in this field. By fostering the exploration of new approaches, this article aims to contribute to the development of high-performance MMMs.

In situ MOF growth

In order to effectively mitigate the agglomeration of a MOF filler within a polymer matrix and enhance interfacial compatibility, an *in situ* MOF growth method within the polymer matrix was proposed to develop a MMM with superior separation performance. This *in situ* growth strategy eliminated the need for separating the MOF from the mother liquor and subsequent drying, thereby not only saving the preparation time and simplifying the production process, but also facilitating cost-effective large-scale industrial production. Furthermore, it prevented the agglomeration of MOF crystals, which could otherwise hinder the dispersion of MOF crystals in the polymer matrix.[17,32,33] The conventional process for preparing MMMs involves the *in situ* growth of MOF crystals within a mixture containing a MOF precursor solution, which comprises metal ions and organic ligands, and a polymer suspension. The presence of a polymer during MOF growth ensures homogeneous dispersion of the MOF filler within the polymer matrix and fosters good interfacial affinity, thanks to the steric hindrance effects and entanglement of the polymer chains.[18,34,35] To streamline this process, a straightforward heat-assisted method for *in situ* MOF growth was introduced for MMM preparation. By casting the mixture of MOF precursor solution and polymer suspension and heating it, both MOF growth and rapid membrane fabrication could be achieved simultaneously (Fig. 1).[14,36] By meticulously controlling the heating temperature, the solvent evaporation rate could be appropriately adjusted to strike a balance between promoting MOF growth

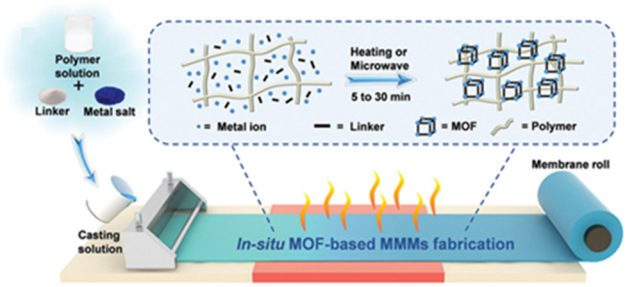

Fig. 1 Schematic diagram of an *in situ* heat-assisted solvent-evaporation method for the fabrication of MOF-based MMMs.[14]

and minimizing defect formation. This *in situ* heat-assisted method was versatile and could be applied to form MMMs with various MOFs, such as HKUST-1, UiO-66, UiO-66-NH_2, Zn–BDC (BDC: 1,4-benzendicarboxylate) and NENU-5. It significantly reduced the tedious preparation steps and allowed producing MMMs with a minimum reaction time of just 5 min. The resulting MMMs exhibited high uniformity, excellent mechanical properties, and adjustable loading and thickness, making them suitable for large-scale production at a rate of approximately 100 m per day – a significant improvement over traditional MOF-based MMM fabrication methods, which often require several days.

To enhance interfacial compatibility and achieve a high MOF loading, a polymer matrix with linker-analogous or reactive groups was introduced.[35,36]By modifying the polymer matrix to graft linker-analogous imidazole groups, MMMs could be formed without any agglomeration, even at a ZIF loading of 40 wt%.[35] For instance, polybenzimidazole (PBI) containing benzimidazole groups facilitated the formation of amorphous ZIFs and improved interfacial compatibility with a 15 wt% ZIF-8 loading (Fig. 2).[36] Remarkably, the ZIF-8 loading could reach an unprecedented 67.2 wt% in a polymer of an intrinsic microporosity (PIM-1) matrix without forming non-selective defects, thanks to the interaction between the CN group of PIM-1 and the NH group of ZIF-8.[37] Notably, the ZIF-8 crystals formed in this system were smaller, with a size reduction of about 50%, indicating the influence of mixed solvents and polymers on MOF nucleation. All the obtained MMMs demonstrated well-dispersed ZIF-8 nanocrystals and excellent interfacial adhesion between the ZIF-8 fillers and the matrix, which effectively facilitated gas transportation. Additionally, a

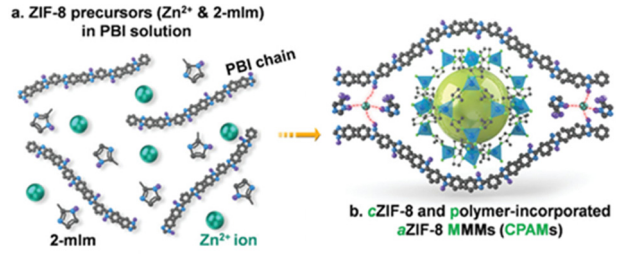

Fig. 2 Schematic illustration of *in situ* growth of cZIF-8 NPs and aZIF-8, including (a) PBI solution containing the precursors for ZIF-8, (b) CPAMs. Adapted from ref. 36 with permission from the John Wiley and Sons.

MOF-induced cross-linked membrane was developed to bolster the mechanical strength, thermal stability, swelling resistance, and separation performance of the MMMs.[38] Zn ions were introduced into a mixture of an imidazole-2-carboxaldehyde ligand solution and a poly(vinyl alcohol) (PVA) suspension to *in situ* synthesize ZIF-90 nanocrystals within the PVA matrix. During subsequent heat treatment, a cross-linking reaction occurred between the hydroxyl groups of PVA and the aldehyde groups of the ligands, resulting in exceptional pervaporation performance.

Another common approach for the preparation of MMMs through *in situ* MOF growth involves the sequential infusion of metal ions and organic ligands into a polymer membrane, thereby facilitating the growth of MOFs within the polymer matrix. It is evident that the order in which the metal ions and organic ligands is introduced can significantly influence the resultant MMM structure. Campbell and colleagues reported that the optimal sequence, involving the initial introduction of a 1,3,5-benzene-tricarboxylic (BTC) ligand solution followed by a Cu ion solution, yielded a HKUST-1-embedded MMM with reduced defects. Conversely, when the Cu ion solution was infused prior to the ligand solution, a brittle HKUST-1 layer formed on top of the polymer membrane.[39] Furthermore, Lim and colleagues discovered that introducing BTC ligands into Cu-alginate spheres resulted in eggshell-shaped HKUST-1 layers on the alginate spheres, whereas introducing Cu ions into BTC-alginate spheres led to the homogeneous dispersion of HKUST-1 crystals within the alginate spheres.[40]

A polymer-modification-enabled MOF formation (PMMOF) strategy was subsequently proposed for the *in situ* formation of ZIF-8 fillers within polyimide-based polymers for MMM preparation.[21,41] The essence of PMMOF is to increase the free volumes of the polymer and modify the polymer chains to accommodate MOF precursors, thereby facilitating *in situ* MOF growth. This process involves four key steps: polymer hydrolysis, ion exchange, ligand treatment, and imidization (Fig. 3). The resultant MMMs exhibited improved ZIF-8 dispersion and interfacial adhesion, with a ZIF-8 loading of 32.9 vol%, and demonstrated higher separation factors compared to those of MMMs prepared by a physical mixing method. Notably, the PMMOF strategy was also found to be applicable to cross-linked polyimide-based matrices, owing to the avoidance of polymer dissolution, which is a limitation of the physical mixing method for the preparation of MMMs containing ZIF-8 and a cross-linked polyimide-based matrix.

In addition to HKUST-1 and ZIF-8, UiO-66-NH_2, known for its high stability, can be synthesized *in situ* within porous polyether sulfonate membranes.[42] Alternatively, metal hydroxides can be used as the metal source for *in situ* MOF growth in MMMs, instead of metal salts.[43] To enhance the affinity between the MOF filler and the membrane, organic ligands were infused into a deposited polyethyleneimine (PEI) layer containing Zn ions, promoting *in situ* Zn-based MOF growth and concurrently tight cross-linking within the MMM.[44,45] This cross-linking arose from coordination bonds between Zn ions from the MOF and NRx groups, as well as hydrogen bonds *via* NH groups from PEI. This approach was effective for both ZIF-8 crystals and 2D ZIF-L crystals.

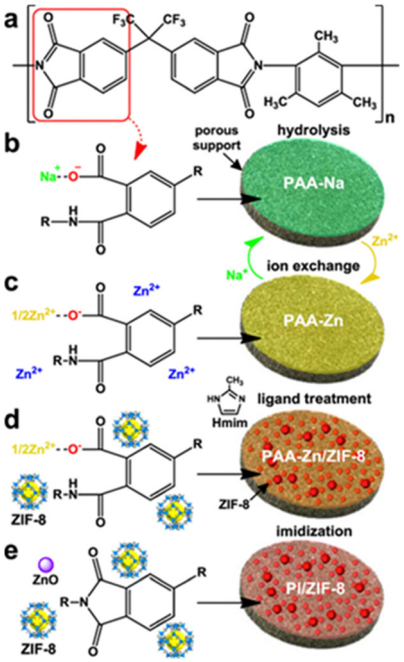

Fig. 3 Schematic of PMMOF using (a) polymer precursor through (b) hydrolysis, (c) ion exchange, (d) ligand treatment, and (e) imidization. Reprinted with permission from ref. 41 Copyright 2019 American Chemical Society.

After proposing the PMMOF strategy, the same research group recently introduced a straightforward one-step method for preparing ZIF-8-embedded MMMs through phase inversion in sync with MOF formation (PIMOF).[46] This approach involved casting a mixture of polymer suspension and Zn ions onto a polymer filter, followed by immersion into a coagulation bath containing 2-methylimidazole (Fig. 4). This process triggered rapid *in situ* MOF growth and simultaneous MMM formation *via* phase inversion. The resultant MMMs were defect-free and featured smaller ZIF-8 fillers (<5 nm) with a high loading capacity exceeding 50 wt%, as well as restricted ligand swing motion, leading to unexpectedly high separation performance for C_3H_6/C_3H_8. A similar non-solvent-induced phase separation process was also employed to form other ZIF-based MMMs, such as ZIF-8/porous polysulfone (PSF) and bimetallic ZnCu-ZIFs/PVDF (PVDF: polyvinylidene fluoride).[47,48] More importantly, the hydrogen bonds between ligands and polymers facilitated homogeneous MOF growth within the MMMs, ensuring good affinity with the polymer matrix. This was achieved by preforming a hybrid membrane containing polymers and ligands, followed by infiltration with Cu and Zn ions. A similar strategy involving the preformation of a hybrid membrane due to the coordination interaction between Zn ions and hydrophilic POEM chains from poly(vinyl chloride)-*graft*-poly(oxyethylene methacrylate) polymer was also applied to form MMMs containing ZIF-8 and amphiphilic graft copolymers, enhancing permeability and selectivity.[49]

It is noteworthy that our group has adopted an innovative spraying technique known as "soft spray" for the *in situ* growth of MOFs within MMMs.[50] In this technique, atomized droplets of metal ions or ligands are gently sprayed onto the liquid surface of a solution containing the other reactants under ambient conditions.[51] The gentle speed of the atomized droplets minimizes turbulence on the liquid surface, thereby promoting directional growth of MOF crystals at the miscible liquid–liquid interface.[52,53] Thanks to its uniform spraying and straightforward operating procedures, the soft spray method has emerged as a promising approach for the preparation of MOF-based materials.[54,55] This "soft spray" technique is suitable for the MOFs synthesized at room temperature, presents potential for large-scale industrial production of MMMs. Utilizing this spraying technique, we have constructed a series of MMMs, including a CuBDC/PVP (PVP: polyvinylpyrrolidone) MMM and a CuBDC/PVP/CB (CB: carbon black) MMM.[23] By spraying Cu ion droplets onto a mixture of BDC solution and polymer suspension, CuBDC crystals are synthesized *in situ* on the liquid surface, subsequently forming a free-standing MMM after drying (Fig. 5). Furthermore, a functionally doped MMM, CuBDC/PVP/CB, can also be fabricated using this rationally designed spray technology. This membrane serves as an efficient reactor for photothermal catalytic CO_2 cycloaddition.

In situ polymerization

In the preparation of MMMs by *in situ* polymerization, a suspension of dispersed MOF crystals and monomers is involved. This method distinguishes itself by achieving a well-dispersed MOF fillers and enhancing interfacial compatibility. Instead of polymers, low molecular weight monomers are easily

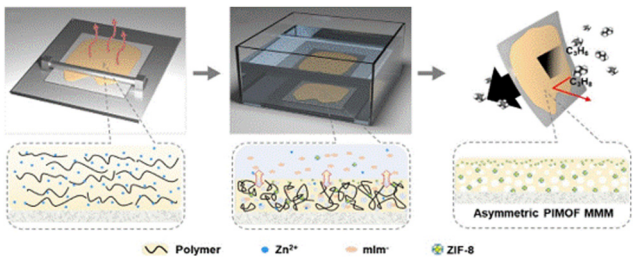

Fig. 4 Schematic illustration of the facile formation of a MMM by the PIMOF process. Adapted from ref. 46 with permission from the Elsevier.

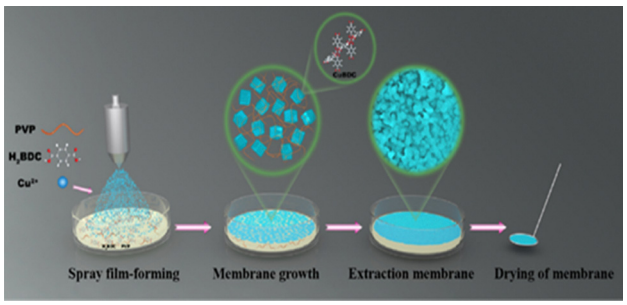

Fig. 5 Schematic illustration of the fabrication of CuBDC/PVP MMMs based on a soft spraying technique. Reprinted with permission from ref. 23 Copyright 2024 American Chemical Society.

dispersed to form a uniform mixture with MOF crystals, which ensures good dispersion of MOF fillers throughout MMMs after *in situ* polymerization. Furthermore, the *in situ* polymerization in the presence of MOF fillers could effectively strengthen filler–polymer adhesion by eliminating interfacial defects, in contrast to the MMMs prepared merely by physical mixing methods, which is crucial for boosting the separation performance of MMMs.

The MMMs prepared by the *in situ* polymerization and thermal imidization of 6FDA-ODA (6FDA: 4,4′-(hexafluoroisopropylidene) diphthalic anhydride; ODA: 4,4′-oxydianiline) in the presence of Cd-6F (with 6FDA serving as the organic ligand) fillers exhibit no interfacial gaps.[56] Notably, the specific interaction between Cd-6F and 6FDA-ODA further contributes to the formation of a superior interface. Similarly, defect-free MMMs were fabricated by conducting UV-irradiated *in situ* polymerization of the polyethylene glycol (PEG) matrix in the presence of ZIF-7-NH_2 nanocrystals. These MMMs demonstrated marked improvements in gas permeability, selectivity, and operational stability.[19] The *in situ* polymerization strategy was also employed for the preparation of MMMs with $Cu_3(BTC)_2$ fillers dispersed within polyetherimide. Notably, a homogeneous dispersion of $Cu_3(BTC)_2$ fillers, loaded at approximately 20 wt%, could be clearly observed within the PEI matrix.[57]

Interfacial polymerization (IP) stands as a prevalent method for *in situ* copolymerization, enabling the fabrication of thin polymer films that are well suited for constructing the polymer matrix of MMMs through an *in situ* polymerization approach.[58] Xu and colleagues have successfully fabricated nanocomposite membranes incorporating MIL-101(Cr) and polyamide (PA) using IP for the purpose of water treatment.[59] This was achieved by immersing a polyether sulfone support in an *m*-phenylenediamine (MPD) solution and subsequently coating it with a mixture of MIL-101(Cr) and trimesoyl chloride (TMC) solution to yield a MIL-101(Cr)/PA membrane (Fig. 6). However, a challenge arose when the concentration of MIL-101(Cr) exceeded 0.1 w/v%, as aggregation of the MOF fillers became difficult to circumvent. To overcome this limitation, amine-modified MOFs were introduced into PA-based MMMs prepared *via* IP, allowing for an increased MOF content.[60] Notably, the MOF filler NH_2-ZIF-8 exhibited the ability to form covalent bonds with TMC and hydrogen bonds with diamines, ensuring the absence of interfacial defects. Compared to MMMs containing ZIF-8, MMMs containing NH_2-ZIF-8 demonstrated superior CO_2 permeability and CO_2/N_2 selectivity. This enhancement was primarily attributed to the improved interfacial compatibility between NH_2-ZIF-8 and PA at the molecular structure level.

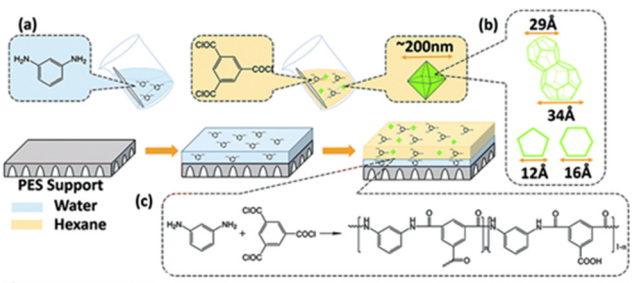

Fig. 6 (a) Schematic representation of preparation of membranes. (b) Schematic representation of the cages and openings of MIL-101(Cr). (c) IP process.[59]

To enhance the compatibility between MOF fillers and the polymer matrix, the approach of *in situ* copolymerization between MOF fillers and monomers or prepolymers was introduced for the preparation of MMMs, a process also known as post-synthetic polymerization of MOFs. To facilitate participation in the *in situ* polymerization of the matrix, vinyl-functionalized MOF fillers were synthesized through post-synthetic modification. UiO-66-type MOFs, renowned for their exceptional thermal stability, were frequently chosen as fillers, as they could maintain their structural integrity during post-synthetic modification and polymerization processes. Specifically, NH_2-UiO-66 was first functionalized with methacrylic anhydride and subsequently polymerized with butyl methacrylate under UV light irradiation.[15] This straightforward polymerization method for MMM preparation was carried out under solvent-free and gentle conditions. The resultant MMM exhibited crack-free, uniform structures and remarkable separation capabilities for Cr(VI) ions.

Furthermore, MMMs containing UiO-66-NH_2 or isopropenyl-functionalized UiO-66-MA as a filler and polyethylene oxide (PEO) as the matrix were developed, following a similar post-synthetic modification and polymerization strategy.[61] UiO-66-MA was obtained by modifying UiO-66-NH_2 with methacrylic anhydride, and the MMM was formed by reacting UiO-66-MA with a mixture of prepolymers under UV light (Fig. 7). While the UiO-66-NH_2/PEO MMM displayed a poor interface, the UiO-66-MA/PEO MMM, characterized by a robust interface due to the copolymerization of UiO-66-MA and the PEO matrix, demonstrated superior gas permeability and unexpectedly suppressed plasticization/swelling behaviour for CO_2 capture.

In addition to isopropenyl-functionalized UiO-66-MA, norbornene-modified UiO-66-NB was synthesized based on the post-synthetic modification of UiO-66-NH_2. This modified MOF was then successfully copolymerized and homogeneously dispersed within a PEG/PPG-PDMS (PPG: polypropylene glycol; PDMS: polydimethylsiloxane) matrix, forming strong covalent bonds between the MOFs and the matrix.[62] The MMM prepared with 3 wt% MOF loading exhibited promising gas separation performance, approaching the 2019 upper bound, and demonstrated antiplasticization and stable antiaging properties.

A novel strategy was also proposed that did not require post-synthetic modification of MOFs, utilizing UiO-66-NH_2 and PIM-1 as the fillers and the matrix, respectively.[20] The amino group of UiO-66-NH_2 reacts with the monomer 1,4-dicyanotetrafluorobenzene (DCTB) (Fig. 8), allowing the MOF fillers to be directly bonded onto the PIM-1 during the polymerization process, resulting in interfacial defect-free MMMs. These MMMs exhibited significantly improved gas separation performance and long-term stability.

It is noteworthy that a high MOF loading could be achieved without the need for a designed covalent bond between the MOF filler and the matrix. For instance, MMMs with a 42%

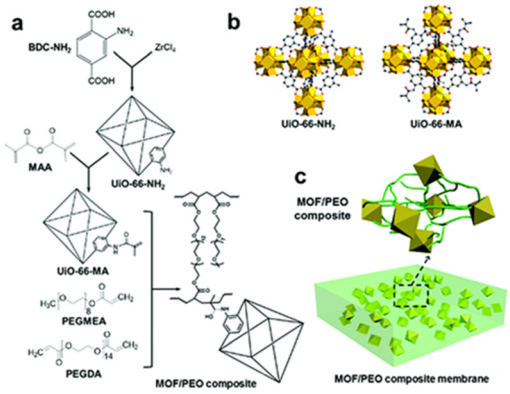

Fig. 7 (a) The synthetic route and structures of UiO-66-NH2, UiO-66-MA and MOF/PEO MMM. (b) Simulated crystal structures of UiO-66-NH2 and UiO-66-MA. (c) 3D structural illustration of the MOF/PEO MMM membrane (octahedrons represent UiO-66-MA particles; cylindrical wires represent PEO molecular chains).[61]

ZIF-8 loading were reported by simultaneously encapsulating ZIF-8 within the matrix during the polymerization of monomers.[63] Furthermore, self-healing MMMs containing UiO-66 with the ability to catalytically degrade chemical warfare agents were fabricated using an *in situ* thiol–ene 'photo-click' polymerization strategy.[64] The self-healing feature of these MMMs is enabled by the reversible hydrolysis of boron-ester conjugates. The resultant MMMs demonstrated exceptional mechanical strength, particularly when Zr(IV)-based MOFs of reduced size were introduced, showing considerable recovery of tensile strength even after two damage healing cycles. Moreover, the chemical warfare agent degradation performance of the MMMs remained consistent even after multiple healing cycles.

The *in situ* polymerization technique was exceptionally conducive to the formation of MMMs incorporating MOFs or MOF composites with specific morphologies. This was facilitated by the mobility of the monomers, which ensured robust affinity with fillers possessing specific morphologies. Specifically, ZIF-8-coated mesoporous silica spheres could be evenly dispersed within a PDMS matrix, achieving MMM formation through *in situ* cross-linking of PDMS prepolymers.[65] These MMMs exhibited enhanced permeability and separation capabilities for ethanol recovery *via* pervaporation. However, when subjected to real-world conditions using actual fermentation froth as the pervaporation feed, a notable decline in permeability and a loss of separation factor were observed.[66] This was primarily attributed to fouling and the instability of ZIF-8 in acidic environments, highlighting the pressing need for MMM fabrication methods that cater to the practical demands of industrial applications. Additionally, MMMs comprising micron-sized hollow ZIF-8 particles were reported using the *in situ* polymerization approach.[67] As the loading of hollow ZIF-8 increased, they formed a continuous and sequentially aligned arrangement across the membrane. This created a low-resistance pathway, facilitating efficient gas transport.

Utilizing the *in situ* polymerization strategy, our research group has reported two studies focused on the construction of asymmetric MMMs. It is noteworthy that the asymmetric structure of these MMMs is induced by the inhomogeneous distribution of fillers. In such asymmetric MMMs, the MOF fillers are concentrated on the membrane surface, effectively minimizing the required MOF loading while achieving sufficient MOF surface coverage to enhance solvent permeance without compromising mechanical properties.[68,69] In contrast, conventional MMMs with symmetric MOF distribution often led to underutilization of MOF fillers. Therefore, asymmetric MMMs have the potential to exhibit improved permeance, high selectivity, and long-term stability.

In the first study, asymmetric MMMs were fabricated through photoinitiated polymerization assisted by the water–liquid interface.[26] A mixture of MOF suspension and monomers was dropped onto a water surface and immediately illuminated with UV light to trigger polymerization and form the MMM at the water–liquid interface (Fig. 9). The polyhedral MOF particles self-assembled at the water–solvent interface to create a MOF-rich surface on one side, while the monomers polymerized at the solvent–air interface to form a polymer-rich surface on the other side. The resulting MMM could achieve a

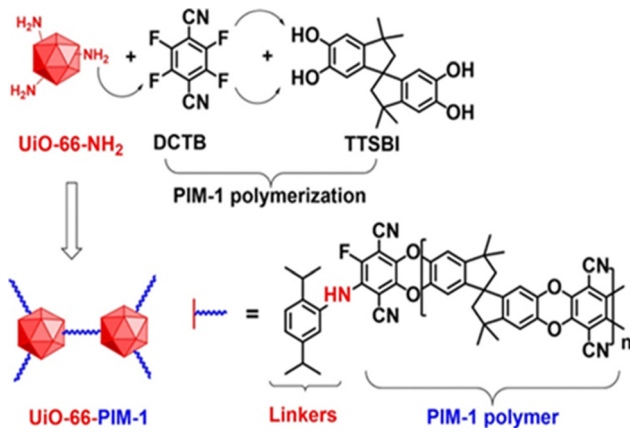

Fig. 8 Cross interface linking between UiO-66-NH2 and PIM-1 obtained during the *in situ* polymerization. Adapted from ref. 20 with permission from the Elsevier.

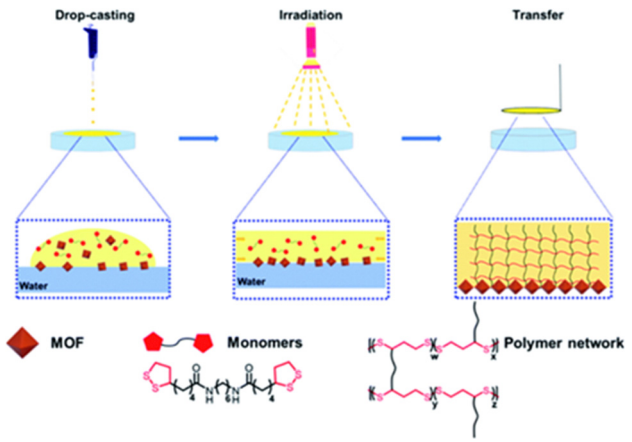

Fig. 9 Illustration of the preparation of oriented MOF polymer films.[26]

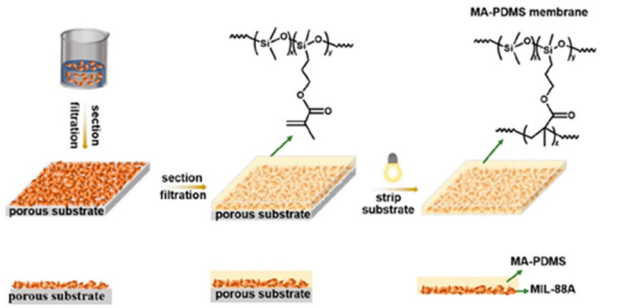

Fig. 10 Schematic drawing of the fabrication of the asymmetrical MIL-88A/MA-PDMS MMM. Reprinted adapted with permission from ref. 27. Copyright 2023 American Chemical Society.

relatively large size of about 24 cm^2, be easily transferred to various substrates, and be adaptable to mixed MOF particles with different sizes and morphologies.

Recently, our group designed an asymmetric MMM as a soft actuating material, featuring a MIL-88A-rich surface on one side and a PDMS-rich surface on the other side.[27] The swellable MIL-88A was selected as the MOF filler to enable the MMM to exhibit reversible folding in response to humidity. The methacrylate-functionalized PDMS (MA-PDMS) was poured onto the surface of the MIL-88A MOF-deposited porous substrate and then subjected to light polymerization to form the MMM (Fig. 10). As MA-PDMS infiltrated the gaps between MOFs, the interfacing MOFs were encapsulated by PDMS, thereby preventing the undesirable delamination commonly observed in traditional bilayer soft actuating materials. Notably, the resultant MMM has the potential to be programmable and capable of reversible 2D-to-3D (3D: three dimensional) shape transformations, making it suitable for precise target object capture and demonstrating significant potential for practical applications.

Obviously, research efforts in MMMs prepared *via in situ* polymerization have primarily concentrated on 3D MOF nanocrystals. However, 2D MOFs have demonstrated distinctive physicochemical properties compared to their 3D counterparts. These unique properties are due to their high aspect ratio, ultrathin thickness, and elevated specific surface area, which offer more accessible active sites. Considering the vast attention garnered by 2D MOFs and their high potential across various applications, our research group has also introduced a typical MMM incorporating 2D MOFs, employing an *in situ* polymerization strategy.[25] Specifically, 2D CuBDC-NH_2 (BDC-NH_2: 2-amino-1,4-benzenedicarboxylate) with reactive amino groups was chosen as the MOF filler. This filler was then reacted with a pre-prepared isocyanate-terminated polyurethane (PU) oligomer to synthesize a CuBDC-NH_2/PU MMM on a supported porous nylon membrane (Fig. 11). This membrane exhibits remarkable efficiency in removing dyes from water.

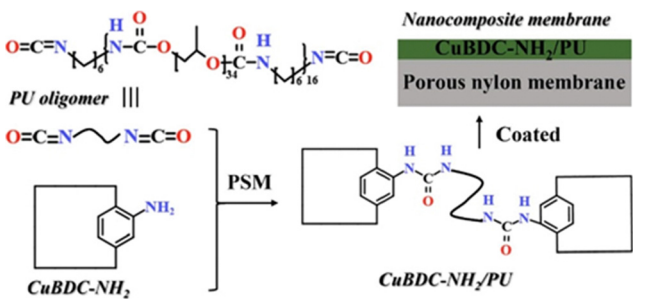

Fig. 11 A schematic illustration of preparing a CuBDC-NH2/PU nanocomposite membrane with an isocyanate-terminated PU oligomer. Adapted from ref. 25 with permission from the Elsevier.

Combined *in situ* methods

Recently, there has been a gradual evolution towards combined *in situ* growth of MOF fillers with *in situ* polymerization of a polymer matrix for the formation of MOF-based MMMs, which notably further simplifies the process and reduces the preparation time compared to individual *in situ* preparation methods. These combined methods can be carried out either sequentially or simultaneously. For the sequential approach, either initial *in situ* MOF growth followed by the subsequent *in situ* polymerization, or initial *in situ* polymerization followed by the subsequent *in situ* MOF growth is available. Subsequently, a simultaneous approach has been proposed, where *in situ* MOF growth and *in situ* polymerization are performed at the same time.

The high-loaded MMMs featuring continuous MOF nanoparticles of highly uniform size and ordered distribution within a cross-linked polymer matrix have been fabricated by sequentially combined *in situ* methods, involving initial thermal polymerization followed by *in situ* MOF growth.[16] Specifically, MOF precursors, consisting of metal ions and organic linkers, are directly introduced into a solvent-free pre-polymerization mixture containing PEG monomers and cross-linkers (Fig. 12). Following *in situ* thermal polymerization, a subsequent thermal treatment at the polymer melting temperature facilitates the rearrangement of MOF precursors within the cross-linked polymer network, leading to the *in situ* formation of continuous MOFs. This innovative *in situ* preparation method can be applied to MMMs containing ZIF-8 and ZIF-7, resulting in excellent interfacial compatibility and achieving a remarkable MOF loading of up to 67.7 wt%. These MMMs exhibit significantly enhanced gas separation performance for CO_2/CH_4 and CO_2/N_2 mixtures.

In a similar approach, a rapid strategy has been proposed for the formation of defect-free, high-loaded MMMs for gas separation using a ZIF-8/PEO system. This strategy combines UV-

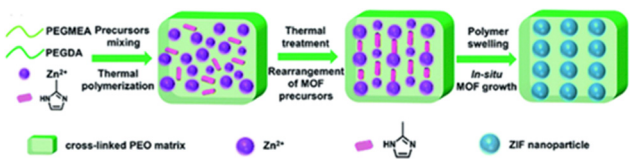

Fig. 12 Schematic illustration of the preparation of a ZIF-based MMM using an *in situ* growth approach.[16]

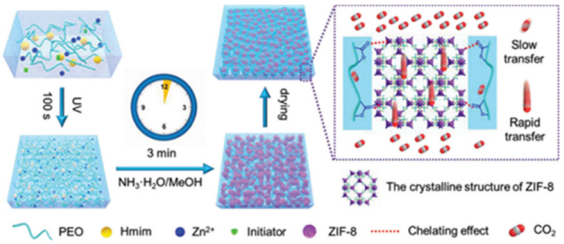

Fig. 13 Schematic illustration of the ZIF/PEO membrane preparation. Adapted from ref. 70 with permission from the John Wiley and Sons.

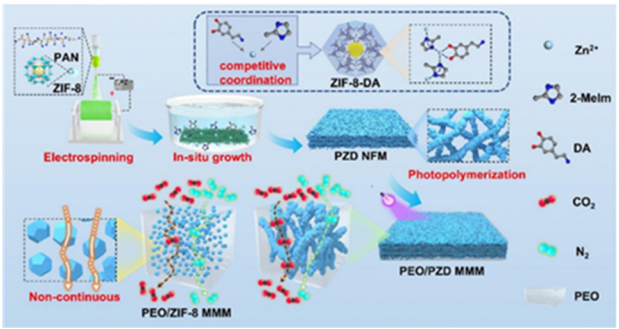

Fig. 14 Schematic diagram of the preparation and separation mechanism of PEO/PZD MMM. Adapted from ref. 74 with permission from the Elsevier.

irradiated polymerization with *in situ* MOF growth.[70] During the fabrication process, a mixture of ZIF-8 precursors and PEO prepolymers is first subjected to UV irradiation for approximately 100 s to form the PEO matrix (Fig. 13). Subsequently, the controlled crystallization of ZIF-8 fillers is achieved using an optimized $NH_3{\cdot}H_2O$/MeOH mixed solvent within 3 min. Uniformly distributed ZIF-8 nanocrystals are observed within the PEO matrix, and the melting interface arising from the interaction between Zn ions and PEO chains is confirmed. The optimized ZIF-8/PEO membrane demonstrates exceptional gas separation performance and long-term operational stability for CO_2/N_2 mixtures.

The realization of sequentially combined *in situ* methods involving a sequence of initial *in situ* MOF growth followed by *in situ* polymerization, offers a particular focus on integrating the IP strategy throughout the process. This is because the monomers easily migrate to the gaps between MOF crystals and then *in situ* polymerized during the IP process to effectively fill these gaps, thereby yielding defect-free MMMs. For instance, HKUST-1 is first grown *in situ* on a cross-linked polyimide (PI) substrate.[71] Subsequently, a PA separation layer is formed through the IP strategy, resulting in the production of an HKUST-1/PA membrane. The abundant amine and amide groups within the cross-linked PI substrate facilitate the uniform distribution of HKUST-1 crystals, thanks to the coordination interactions between Cu ions and these functional groups. Similarly, Fe(BTC)/PA MMMs are obtained through a comparable process of *in situ* MOF growth and IP.[72] After coating a PSF substrate with an Fe^{3+}–polyphenolic complex, Fe(BTC) crystals are synthesized *in situ* by introducing H_3BTC ligands. A PA matrix is then prepared through IP to fill the gaps and produce the Fe(BTC)/PA MMM. The pre-coating of the Fe^{3+}–polyphenolic complex ensures well-dispersed Fe(BTC) formation on the PSF substrate. Using analogous methods, UiO-66-NH_2 nanoparticles are synthesized and loaded onto the surface of a nylon membrane.[73] A dense PA layer was then constructed through IP to mend the gaps between the MOF nanoparticles. Notably, UiO-66-NH_2 fillers actively participate in the IP process, which is driven by reactions between the amino groups of UiO-66-NH_2 and the acyl chloride of TMC. This interaction effectively prevents the agglomeration of MOFs and reduces interfacial defects. Consequently, these MMMs exhibit improved nanofiltration performance.

To further enhance both the mechanical robustness and gas separation capabilities, a dopamine (DA)-assisted MOF growth strategy was employed to create MMMs featuring bi-continuous MOF transfer pathways.[74] A polyacrylonitrile@ZIF-8 (PAN@ZIF-8) nanofiber mat (NFM) was first prepared through electrospinning (Fig. 14). Subsequently, ZIF-8 was *in situ* grown on the surface of the PAN@ZIF-8 NFM using the functional small molecule DA, resulting in the formation of a PZD NFM. The abundant hydroxy and amino groups present in DA facilitated coordination interactions with Zn ions, thereby promoting the heterogeneous nucleation and growth of ZIF-8 on the NFM. The resultant PEO/PZD MMM exhibited a bi-continuous ZIF-8 transfer pathway with a ZIF-8 loading of 72.41 vol% and exceptional interfacial compatibility. This unique structure revealed outstanding mechanical properties and gas separation performance for CO_2/N_2 mixtures, surpassing the 2019 McKeown upper bound.

The simultaneously combined *in situ* methods induce *in situ* MOF growth and *in situ* polymerization at the same time. This simultaneously combined *in situ* approach could be used to manufacture ZIF-8/PDMS MMMs with exceptional permeability.[75] During the membrane preparation process, two solutions were coated onto the surface of a PVDF-supported PDMS layer: one containing PDMS, tetraethyl orthosilicate, and Zn ions, and the other containing PDMS, dibutyltin dilaurate, and 2-methylimidazole (Fig. 15). The thermal curing process subsequently triggered both the growth of ZIF-8 and the polymerization of PDMS

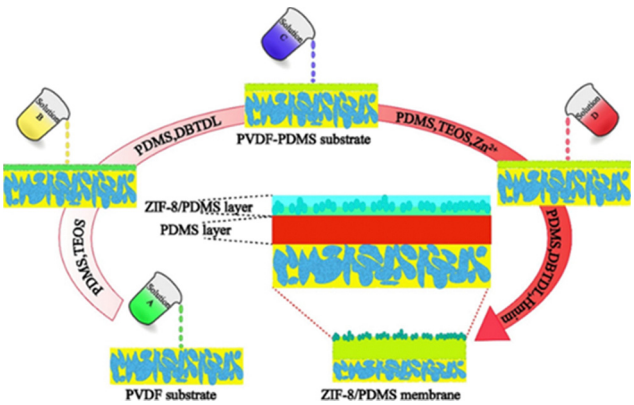

Fig. 15 Schematic diagram of ZIF-8/PDMS MMM prepared by an *in situ* synthesis method. Adapted from ref. 75 with permission from the Elsevier. American Chemical Society.

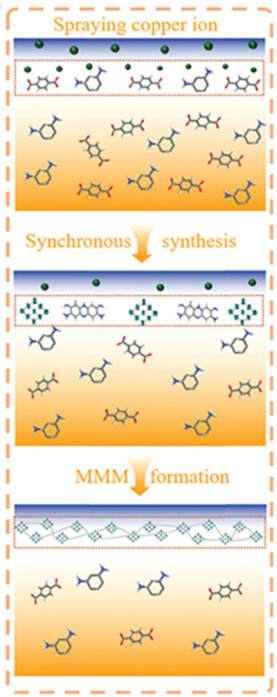

Fig. 16 Formation mechanism of a simultaneously combined *in situ* method for CuBDC/PmPD MMMs through soft spray. Adapted from ref. 24 with permission from the John Wiley and Sons.

simultaneously, aiding in the formation of highly effective active layers. These layers included a continuous PDMS layer and a ZIF-8/PDMS layer, providing additional permeable diffusion channels. Consequently, the resultant defect-free MMM exhibited a maximum flux of 2046.3 g m^{-2} h^{-1} without compromising the separation factor for *n*-butanol pervaporation recovery.

Utilizing simultaneously combined *in situ* methods, our research group has devised a straightforward "soft spray" strategy for constructing high-loaded MMMs with oriented 2D CuBDC MOFs.[24] In this approach, Cu ion droplets are uniformly sprayed onto the surface of a mixture containing BDC ligands and MPD monomers under ambient conditions. Subsequently, a large-scale CuBDC/poly(*m*-phenylenediamine) (CuBDC/PmPD) MMM is rapidly fabricated at the air–liquid interface. The growth of CuBDC crystals occurred simultaneously with stimulated polymerization triggered by the metal ions (Fig. 16). The resultant MMM exhibits a defect-free structure even on a relatively large scale, featuring an oriented arrangement of 2D CuBDC throughout the membrane. This unique structure contributes to impressive separation performance in terms of Li(I) permeability and Li(I)/Mg(II) selectivity. Furthermore, the MMM also demonstrates exceptional solar water evaporation performance, making it a versatile material for various applications.

In situ post-treatment

Apart from the preparation of MMMs through *in situ* MOF growth or/and *in situ* polymerization, various interfacial design strategies have garnered significant attention, particularly those employing *in situ* post-treatment of MMMs. These strategies are highly effective in enhancing the interfacial compatibility between the MOF filler and the polymer matrix. Recently, a variety of *in situ* post-treatment techniques have been reported, including *in situ* postsynthetic modification and ligand exchange, *in situ* thermal annealing, *in situ* thermal cross-linking, *in situ* etching, *in situ* MOF amorphization, and *in situ* aminolysis.

An *in situ* postsynthetic modification and exchange of ligands from MOF fillers can be achieved within MMMs. For instance, approximately 33% of the BDC ligands in UiO-66 were exchanged for BDC-NH_2 to form UiO-66-NH_2 within a PVDF matrix. Furthermore, nearly 75% of UiO-66-NH_2 was converted to UiO-66-AM1 after modification of BDC-NH_2 with acetic anhydride.[76] These findings offer promising avenues for the further customization and enhancement of MMMs through postsynthetic modifications.

A thermal annealing operation was conducted to optimize the interface morphology of the MMM, thereby enhancing its separation performance and mechanical stability.[77] Specifically, the MMM was formulated by incorporating ZIF-8 nanoplates into a Matrimid matrix, followed by a thermal annealing process at temperatures ranging from 160 °C to 320 °C for a duration of 8 h. Upon completion of the annealing process, no significant damage was observed in either the ZIF-8 fillers or the Matrimid matrix. Instead, a robust and tight connection between the ZIF-8 fillers and the Matrimid matrix, characterized by a reduction in interface defects, became evident. This positive outcome could be attributed to the rearrangement of polymer chains during the thermal annealing process. Furthermore, the MMMs exhibited a notable increase in glass transition temperature compared to the pristine Matrimid membrane, which indicated interactions between the ZIF-8 and Matrimid components and confirmed the presence of good interfacial compatibility. Consequently, the thermally annealed ZIF-8-Matrimid MMMs demonstrated an exceptional H_2/CO_2 selectivity of 10.3, a hydrogen permeability of 330.1 barrer, and sustained stability over a period of 400 h testing.

The interfacial force can be significantly enhanced through *in situ* thermal cross-linking.[29] Specifically, desolventized membranes composed of NH_2-MIL-53 fillers, PA, and polyamic acid were fabricated and subsequently thermally treated in an argon atmosphere. During the *in situ* post-thermal treatment, an imidization reaction took place between the amino groups of NH_2-MIL-53 and the carboxylic groups of polyamic acid, accompanied by the formation of hydrogen bonds between NH_2-MIL-53 and PA (Fig. 17). Hence, the MMM with a 30 wt% MOF loading exhibited an exceptional hydrogen permeability of 384.1 barrer and a H_2/CO_2 selectivity of 16.7, surpassing the 2008 Robeson upper bound. This outstanding performance can be attributed to the improved interfacial compatibility in the MMM, achieved through *in situ* interfacial cross-linking.

A unique *in situ* etching approach was devised to construct MMMs with nearly defect-free interfaces.[78] The choice of materials included ZIF-8 and PI functionalized with acid groups

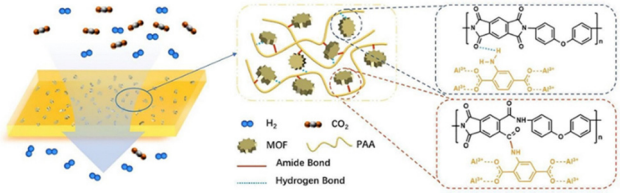

Fig. 17 Schematic illustration of the formation of the interfacial interaction in MMMs. Adapted from ref. 29 with permission from the Elsevier. American Chemical Society.

(PI-COOH), to forge dense MMMs. During the membrane formation process, ZIF-8 underwent *in situ* etching by the carboxylic acid groups of PI-COOH, while the unsaturated Zn sites on the ZIF-8 filler surface coordinately interacted with PI-COOH (Fig. 18). This interaction notably decreased the number of interfacial defects within the MMM. Furthermore, the pathway for gas transport through the MMM shifted from bypassing to interpenetrating, yielding exceptional gas permeability and selectivity for the separation of H_2/N_2, H_2/CH_4, and O_2/N_2 mixtures. These performance metrics approached the 2015 Robeson upper bound, highlighting the remarkable efficacy of the proposed *in situ* etching strategy.

In contrast to MMMs formed with pristine MOF crystals, MOF glass-based MMMs have demonstrated exceptional gas separation capabilities. Notably, MOF glasses are often synthesized through melt-quenching, and several MMMs incorporating MOF glass have been reported using *in situ* thermal treatment methods. The benefits of employing thermal treatment for fabricating MOF glass-based MMMs include ease of processing, enhanced interfacial compatibility of the MMM, and the potential for achieving high-loaded MMMs with large-scale production for practical applications.

A thermal treatment was conducted on MMMs comprising ZIF-62 fillers and a 6FDA-DAM (DAM: 2,4,6-trimethyl-*m*-phenyl enediamine) matrix at 390 °C under an argon atmosphere, resulting in the formation of a ZIF-62 glass phase within the polymer matrix (Fig. 19).[28] By heating ZIF-62 to its melting temperature, the crystals transitioned into a molten liquid state, facilitating the shaping of macroscopic structures. This transition provides an opportunity to use the liquid state of ZIF-62 to tailor the MOF surface and MOF–polymer interface within the MMM. Consequently, the voids at the MOF–polymer interface were filled by the liquid phase of ZIF-62 through *in situ* melting. This was confirmed through a combination of focused ion beam scanning electron microscopy, thermal characterization, and membrane separation tests.

Subsequently, PBI and PIM-1 known for their exceptional thermal stability (thermal decomposition temperature exceeding 520 °C) were chosen to be hybridized with ZIF-62 to produce ZIF-62 glass-based MMMs. Similarly, an enhancement in interfacial compatibility of MMMs with high MOF loading was observed for MMMs composed of a ZIF-62 filler and a PBI polymer matrix through an *in situ* heating process.[79] After heating at 460 °C in a vacuum, the molten liquid-phase state of ZIF-62 effectively filled the interfacial defects of the MMM, leading to the formation of a continuous ZIF-62 glass phase and exhibiting excellent dispersibility. With 45 wt% ZIF-62 glass, the MMM exhibited a high H_2 permeability of 459 barrer, along with impressive H_2/CO_2 and H_2/CH_4 selectivities of 23 and 57, respectively. Additionally, the ZIF-62 glass/PBI MMMs demonstrated enhanced stability under gas pressures ranging from 1 to 5 bar and after 120 h of testing. For PIM-1, a partial self-cross-linking reaction occurs during heating, which increases the overall free volume due to chain rearrangement and inefficient packing when subjected to appropriate thermal treatment.[80] Consequently, the MMM composed of the ZIF-62 filler and PIM-1 matrix exhibited the elimination of interfacial non-selective voids and a simultaneous increase in the PIM-1 free volume after thermal treatment at 420 °C under an argon atmosphere.[81] The resulting ZIF-62 glass/PIM-1 MMM with 30% MOF loading significantly enhanced both permeability and selectivity for CO_2/CH_4 separation, achieving a CO_2/CH_4 selectivity of 67 and a CO_2 permeability of 5914 barrer, surpassing the 2019 upper bound.

In addition to ZIF-62, the *in situ* amorphization of ZIF-8 fillers within the Matrimid matrix was achieved through thermal treatment at 350 °C in air.[82] Simultaneously, thermo-oxidative cross-linking of the MMM was realized using the proposed cross-linking mechanism for the Matrimid matrix

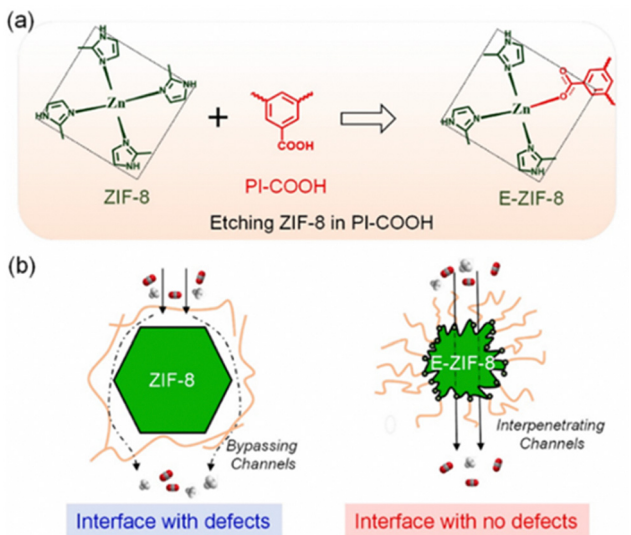

Fig. 18 Schematic illustration of (a) chemical reaction between ZIF-8 and PI-COOH to give rise to the etching of ZIF-8 nanoparticles in the PI-COOH matrix and (b) interface structure and gas transportation in ZIF-8 and E-ZIF-8 based hybrid membranes. Adapted from ref. 78 with permission from the Elsevier.

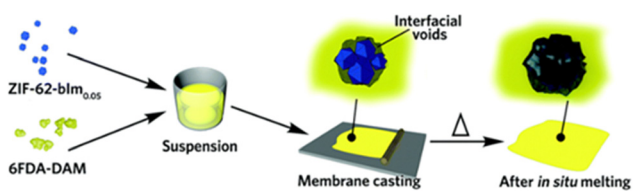

Fig. 19 Scheme of the preparation of glass ZIF-based mixed-matrix membranes.[28]

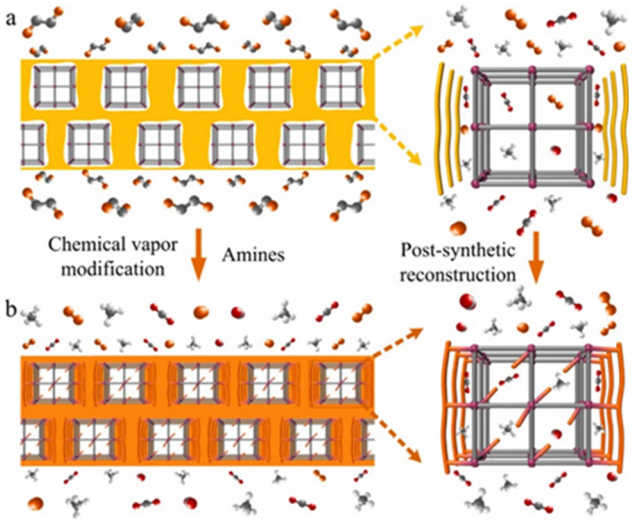

Fig. 20 Post-synthetic reconstruction of MMMs. (a) Schematic of chemical vapor deposition of defect MOFPIM MMMs to reduce nonselective transports through *in situ* aminolysis. (b) Schematic of defect-free MOFIM-A MMMs for selective transport of various gases. Adapted from ref. 83 with permission from the Elsevier.

and ZIF-8 fillers, based on the FTIR results. This thermal treatment was employed to develop MMMs with a high loading of up to 40 wt% ZIF-8. The thermally induced amorphous ZIF-8 and the additional polymer cross-linking effectively enhanced filler-polymer adhesion, leading to an ultra-high selectivity for separating CO_2 from CH_4. Notably, the MMMs exhibited significantly increased stability and plasticization resistance at high pressures at high pressure up to 40 bar.

A post-synthetic reconstruction method for MMMs has been reported, involving *in situ* aminolysis through chemical vapor deposition under mild conditions, with the aim of enhancing their gas separation performance.[83] ZIF-8 fillers and the PIM-1 matrix were chosen to form the MMMs, due to their hydrophobic nature and the favorable interactions between the zinc centers of ZIF-8 and the oxygen heterocycles of PIM-1. After undergoing chemical vapor deposition with ethylenediamine (EDA), the MMMs exhibited a robust phase-interfacial boundary, resulting from the tight interfacial adhesion achieved through *in situ* aminolysis (Fig. 20). This process allowed for the substitution and grafting of EDA onto PIM-1, chelation at the zinc centers of ZIF-8, and insertion within the frameworks. These modifications effectively strengthened the compatibility of the MMMs, regulated their transport properties, and enhanced preferential adsorption. Consequently, the MMM subjected to *in situ* aminolysis demonstrated improved anti-aging properties and enhanced separation performance for CO_2/N_2 and CH_4/N_2 gas pairs.

Conclusions

In situ strategies have been employed to synthesize MOF-based MMMs utilizing different types of MOF fillers and polymer matrixes. These approaches encompass *in situ* MOF growth, *in situ* polymerization of polymer matrixes, and combined *in situ* methods. *In situ* MOF growth could simplify the preparation process, mitigate the aggregation of MOF particles due to the presence of polymer chains and result in improved interfacial affinity. In addition to a simple heat-assisted method for MMM formation, polymers with linker-analogous groups, reactive groups, or pre-mixed metal ions have been introduced to improve interfacial compatibility through cross-linking. Furthermore, a non-solvent induced phase separation process has been integrated with *in situ* MOF growth to construct MMMs in a one-step approach. Noteworthily, the selected polymer should be stable enough during the MOF growth, especially for the MOFs formed by solvothermal and hydrothermal synthesis methods.

Besides similar simplified preparation processes, defect-free MMMs are easily formed through *in situ* polymerization due to the mobility of monomers, which ensures good affinity between the polymer and the MOF, even in unusual hollow morphologies or composite structures. IP has become a common method for *in situ* polymerization to fabricate MOF-based MMMs. In addition, copolymerization between MOFs and monomers or prepolymers can be readily achieved by modifying MOFs with active groups to enhance interfacial affinity. Noteworthily, the stability of MOFs is required for the *in situ* polymerization and a modifiable MOF is suitable for anticipating copolymerization with polymers.

The combination of *in situ* MOF growth and *in situ* polymerization has been applied to the fabrication of MOF-based MMMs, which can be performed either sequentially or simultaneously. These combined *in situ* methods further simplify the fabrication process and can be completed more rapidly than a single *in situ* method. However, selection of polymers and MOFs is limited by the required stability and reactivity, especially for the simultaneous combined *in situ* methods.

In situ post-treatment of MMMs has emerged as an effective way to reduce defects and enhance interfacial compatibility. *In situ* thermal annealing and *in situ* MOF amorphization exploit the mobility of the polymer and molten MOF, respectively, to repair interfacial defects. *In situ* thermal cross-linking, *in situ* etching, and *in situ* aminolysis can improve filler–polymer adhesion by forming covalent or non-covalent interactions between MOFs and polymers. And the *in situ* postsynthetic modification and ligand exchange offer promising avenues for further customization of MMMs.

According to the *in situ* preparation schemes, our group has developed a ''soft spray'' technique for *in situ* MOF growth to prepare functional MMMs, even with additional dopants. Moreover, the ''soft spray'' technique was also applied to the simultaneous combined *in situ* method for successful construction of high-loaded 2D MOF-based MMMs. The devised ''soft spray'' technique is suitable for the MOFs synthesized at room temperature, and has potential for large-scale industrial production of MMMs. Moreover, our group has innovatively constructed asymmetric MMMs through an *in situ* polymerization strategy with the assistance of the water–liquid interface and sequential deposition of MOFs and subsequent monomers. The asymmetric MMMs offer new ideas for the design of MMMs with high performance for practical applications.

Although the industrial production of MOF-based MMMs still faces challenges, the high application potential and industrial prospects of MOF-based MMMs prepared through *in situ* strategies are undeniable. This feature article summarizes recent innovations in the *in situ* strategies for constructing MOF-based MMMs and encourages the exploration of new approaches to achieve high-performance MMMs.

Author contributions

Liying Zhang: conceptualisation, investigation, visualisation, supervision, funding acquisition, writing – original draft, writing – review and editing, and project administration; Yuxin He: investigation, visualisation, writing – original draft, and writing – review and editing; Yu Fu: conceptualisation, supervision, funding acquisition, writing – review and editing, and project administration.

Data availability

No primary research results, software or code have been included and no new data were generated or analysed as part of this feature article.

Conflicts of interest

There are no conflicts to declare.

Acknowledgements

This work was supported by the Natural Science Foundation Plan of Liaoning Province (2024-MSBA-45), the National Natural Science Foundation of China (22175030), and Open Project of State Key Laboratory of Supramolecular Structure and Materials (sklssm202306). We also specially thank the Analytical and Testing Center at Northeastern University for experimental and instrumental support.

Notes and references

1 J. Dechnik, J. Gascon, C. J. Doonan, C. Janiak and C. J. Sumby, *Angew. Chem., Int. Ed.*, 2017, **56**, 9292–9310.
2 M. Wang, Z. Wang, S. Zhao, J. X. Wang and S. C. Wang, *Chin. J. Chem. Eng.*, 2017, **25**, 1581–1597.
3 L. Q. Hu, K. Clark, T. Alebrahim and H. Q. Lin, *J. Membr. Sci.*, 2022, **644**, 120140.
4 K. Xu, S. T. Zhang, X. L. Zhuang, G. X. Zhang, Y. J. Tang and H. Pang, *Adv. Colloid Interface Sci.*, 2024, **323**, 103050.
5 L. M. Robeson, *J. Membr. Sci.*, 2008, **320**, 390–400.
6 H. Furukawa, K. E. Cordova, M. O'Keeffe and O. M. Yaghi, *Science*, 2013, **341**, 1230444.
7 Z. Chen, H. Jiang, M. Li, M. O'Keeffe and M. Eddaoudi, *Chem. Rev.*, 2020, **120**, 8039–8065.
8 H. R. Zheng, D. Deng, X. R. Zheng, Y. B. Chen, Y. Bai, M. J. Liu, J. B. Jiang, H. T. Zheng, Y. C. Wang, J. X. Wang, P. Y. Yang, Y. Xiong, X. Xiong and Y. P. Lei, *Nano Lett.*, 2024, **24**, 4672–4681.
9 H. R. Zheng, S. B. Wang, S. J. Liu, J. Wu, J. P. Guan, Q. Li, Y. C. Wang, Y. Tao, S. Y. Hu, Y. Bai, J. X. Wang, X. Xiong, Y. Xiong and Y. P. Lei, *Adv. Funct. Mater.*, 2023, **33**, 2300815.
10 W. X. He, X. Y. Li, X. Y. Dai, L. Shao, Y. Fu, D. Xu and W. Qi, *Angew. Chem., Int. Ed.*, 2024, **63**, e202411539.
11 R. J. Lin, B. V. Hernandez, L. Ge and Z. H. Zhu, *J. Mater. Chem. A*, 2018, **6**, 293–312.
12 Q. H. Qian, P. A. Asinger, M. J. Lee, G. Han, K. Ma. Rodriguez, S. Lin, F. M. Benedetti, A. X. Wu, W. S. Chi and Z. P. Smith, *Chem. Rev.*, 2020, **120**, 8161–8266.
13 M. A. Aroon, A. F. Ismail, T. Matsuura and M. M. Montazer-Rahmati, *Sep. Purif. Technol.*, 2010, **75**, 229–242.
14 G. K. Gao, Y. R. Wang, H. J. Zhu, Y. F. Chen, R. X. Yang, C. Jiang, H. Y. Ma and Y. Q. Lan, *Adv. Sci.*, 2020, **7**, 2002190.
15 Y. Y. Zhang, X. Feng, H. W. Li, Y. F. Chen, J. S. Zhao, S. Wang, L. Wang and B. Wang, *Angew. Chem., Int. Ed.*, 2015, **54**, 4259–4263.
16 L. Ma, F. Svec, Y. Q. Lv and T. W. Tan, *J. Mater. Chem. A*, 2019, **7**, 20293–20301.
17 R. Zhang, S. L. Ji, N. X. Wang, L. Wang, G. J. Zhang and J. R. Li, *Angew. Chem., Int. Ed.*, 2014, **53**, 9775–9779.
18 C. W. Zhao, J. P. Ma, Q. K. Liu, X. R. Wang, Y. Liu, J. Yang, J. S. Yang and Y. B. Dong, *Chem. Commun.*, 2016, **52**, 5238–5241.
19 L. Xiang, L. Q. Sheng, C. Q. Wang, L. X. Zhang, Y. C. Pan and Y. S. Li, *Adv. Mater.*, 2017, **29**, 1606999.
20 N. Tien-Binh, D. Rodrigue and S. Kaliaguine, *J. Membr. Sci.*, 2018, **548**, 429–438.
21 S. Park and H. K. Jeong, *Membranes*, 2022, **12**, 964.
22 B. Zhang, J. Y. Chen and Y. Fu, *Langmuir*, 2022, **38**, 13635–13646.
23 B. Zhang, X. Cheng, K. Cheng, Y. Fu and W. Z. Li, *Inorg. Chem.*, 2024, **63**, 1102–1108.
24 B. Zhang, X. Y. Dai, N. N. Wei, X. C. Cui, F. Q. Fan, J. D. Zhang, D. L. Zhang, F. B. Meng, W. Qi and Y. Fu, *Small*, 2024, **20**, 2305688.
25 M. C. Li, L. Y. Zhang, X. H. Wang, X. M. Zhang, T. Q. Wang, F. Q. Fan and Y. Yu, *Inorg. Chem. Commun.*, 2022, **146**, 110137.
26 F. Q. Fan, Z. H. Zhang, Q. Q. Zeng, L. Y. Zhang, X. M. Zhang, T. Q. Wang and Y. Fu, *RSC Adv.*, 2022, **12**, 19406–19411.
27 B. Zhang, X. C. Cui, W. X. He, L. Shao, T. Q. Wang, F. B. Meng and Y. Fu, *ACS Appl. Polym. Mater.*, 2023, **5**, 7090–7097.
28 R. J. Lin, J. W. Hou, M. R. Li, Z. K. Wang, L. Ge, S. C. Li, S. Smart, Z. H. Zhu, T. D. Bennett and V. Chen, *Chem. Commun.*, 2020, **56**, 3609–3612.
29 Y. Jia, P. X. Liu, Y. B. Liu, D. Zhang, Y. Ning, C. Xu and Y. Zhang, *Fuel*, 2023, **339**, 126938.
30 B. Seoane, V. Sebastián, C. Téllez and J. Coronas, *CrystEngComm*, 2013, **15**, 9483–9490.
31 M. S. Maleh and A. Raisi, *Chem. Eng. Res. Des.*, 2022, **186**, 266–275.
32 N. Missaoui, G. Chaplais, L. Josien, L. Michelin, G. Schrodj and A. H. Said, *Polym. Eng. Sci.*, 2020, **60**, 464–473.
33 W. Wang, Y. P. Shi, P. Zhang, Z. C. Zhang and X. Xu, *J. Phys. Chem. Solids*, 2022, **171**, 110865.
34 A. M. Marti, S. R. Venna, E. A. Roth, J. T. Culp and D. P. Hopkinson, *ACS Appl. Mater. Interfaces*, 2018, **10**, 24784–24790.
35 S. Shahid, K. Nijmeijer, S. Nehache, I. Vankelecom, A. Deratani and D. Quemener, *J. Membr. Sci.*, 2015, **492**, 21–31.
36 L. Q. Hu, V. T. Bui, S. Pal, W. J. Guo, A. Subramanian, K. Kisslinger, S. H. Fan, C.-Y. Nam, Y. F. Ding and H. Q. Lin, *Small*, 2022, **18**, 2201982.
37 S. S. He, B. Zhu, X. Jiang, G. Han, S. W. Li, C. H. Lau, Y. D. Wu, Y. Q. Zhang and L. Shao, *Proc. Natl. Acad. Sci. U. S. A.*, 2022, **119**, 2114964119.
38 Z. Wei, Q. Liu, C. L. Wu, H. Y. Wang and H. Wang, *Sep. Purif. Technol.*, 2018, **201**, 256–267.
39 J. Campbell, R. P. Davies, D. C. Braddock and A. G. Livingston, *J. Mater. Chem. A*, 2015, **3**, 9668–9674.
40 J. Lim, E. J. Lee, J. S. Choi and N. C. Jeong, *ACS Appl. Mater. Interfaces*, 2018, **10**, 3793–3800.
41 S. Park, M. R. A. Hamid and H. K. Jeong, *ACS Appl. Mater. Interfaces*, 2019, **11**, 25949–25957.
42 Z. W. Li, W. T. Zhang, M. Tao, L. G. Shen, R. J. Li, M. J. Zhang, Y. Jiao, H. C. Hong, Y. C. Xu and H. J. Lin, *Chem. Eng. J.*, 2022, **435**, 134804.
43 Y. Guo, Y. L. Ying, Y. Y. Mao, X. S. Peng and B. L. Chen, *Angew. Chem., Int. Ed.*, 2016, **55**, 15120–15124.
44 L. B. Yang, Z. Wang and J. L. Zhang, *J. Membr. Sci.*, 2017, **532**, 76–86.
45 S. Y. Li, L. D. Tu, Y. Q. Lu, M. J. Lin, J. M. Ma, C. J. Bai, C. J. Gao and L. X. Xue, *Sep. Purif. Technol.*, 2023, **324**, 124435.
46 Y. Y. Hua, S. Park, G. M. Choi, H. J. Jung, K. Y. Cho and H. K. Jeong, *Chem. Eng. J.*, 2023, **466**, 143048.
47 H. Yu, D. J. Cai, S. Y. Li, C. J. Gao and L. X. Xue, *J. Membr. Sci.*, 2023, **666**, 121136.

48 X. Yang, X. Y. Chen, X. L. Su, A. Cavaco-Paulo, H. B. Wang and J. Su, *Sep. Purif. Technol.*, 2024, **344**, 127221.
49 C. S. Lee, N. U. Kim, B. J. Park and J. H. Kim, *Sep. Purif. Technol.*, 2020, **253**, 117514.
50 B. Zhang, J. Y. Chen and Y. Fu, *Langmuir*, 2022, **38**, 13635–13646.
51 S. Wang, J. C. Ma, X. Zhai, X. M. Zhang, F. Q. Fan, T. Q. Wang, Y. N. Li, L. Y. Zhang and Y. Fu, *Langmuir*, 2020, **36**, 7392–7399.
52 X. J. Bai, Y. N. Li, X. M. Yang, M. Y. Zhang, L. Shao, B. Zhang, T. Q. Wang, X. M. Zhang, L. Y. Zhang, Y. Fu and W. Qi, *Chem. Commun.*, 2019, **55**, 9343–9346.
53 X. J. Bai, D. Chen, L. L. Li, L. Shao, W. X. He, H. Chen, Y. N. Li, X. M. Zhang, T. Q. Wang, Y. Fu and W. Qi, *ACS Appl. Mater. Interfaces*, 2018, **10**, 25960–25966.
54 X. J. Bai, X. Y. Lu, R. Ju, H. Chen, L. Shao, X. Zhai, Y. N. Li, F. Q. Fan, Y. Fu and W. Qi, *Angew. Chem., Int. Ed.*, 2021, **60**, 701–705.
55 X. J. Bai, H. Chen, Y. N. Li, L. Shao, J. C. Ma, L. L. Li, J. Y. Chen, T. Q. Wang, X. M. Zhang, L. Y. Zhang, Y. Fu and W. Qi, *New J. Chem.*, 2020, **44**, 1694–1698.
56 R. J. Lin, L. Ge, L. Hou, E. Strounina, V. Rudolph and Z. H. Zhu, *ACS Appl. Mater. Interfaces*, 2014, **6**, 5609–5618.
57 M. Hegde, S. Shahid, B. Norder, T. J. Dingemans and K. Nijmeijer, *Polymer*, 2015, **81**, 87–98.
58 M. F. Jimenez-Solomon, Q. L. Song, K. E. Jelfs, M. Munoz-Ibanez and A. G. Livingston, *Nat. Mater.*, 2016, **15**, 760–767.
59 Y. Xu, X. L. Gao, Q. Wang, X. Y. Wang, Z. Y. Ji and C. J. Gao, *RSC Adv.*, 2016, **6**, 82669–82675.
60 S. W. Yu, S. C. Li, S. L. Huang, Z. H. Zeng, S. Cui and Y. Liu, *J. Membr. Sci.*, 2017, **540**, 155–164.
61 X. Jiang, S. W. Li, S. S. He, Y. P. Bai and L. Shao, *J. Mater. Chem. A*, 2018, **6**, 15064–15073.
62 I. Hossain, A. Husna, S. Chaemchuen, F. Verpoort and T. H. Kim, *ACS Appl. Mater. Interfaces*, 2020, **12**, 57916–57931.
63 R. Y. Li, J. P. Chen and V. Freger, *J. Membr. Sci.*, 2023, **671**, 121357.
64 P. Mondal and S. M. Cohen, *Chem. Sci.*, 2022, **13**, 12127.
65 P. V. Naik, L. H. Wee, M. Meledina, S. Turner, Y. B. Li, G. V. Tendeloo, J. A. Martensa and I. F. J. Vankelecom, *J. Mater. Chem. A*, 2016, **4**, 12790–12798.
66 C. V. Goethem, P. V. Naik, M. V. de Velde, J. V. Durme, A. Verplaetse and I. F. J. Vankelecom, *Membranes*, 2023, **13**, 863.
67 W. J. Zheng, R. Ding, Z. H. Li, X. H. Ruan, Y. Dai, M. Yu, X. C. Li, X. M. Yan, X. B. Jiang, X. J. Zhang and G. H. He, *Chem. Eng. J.*, 2024, **490**, 151639.
68 R. Hardian, J. T. Jia, A. Diaz-Marquez, S. Naskar, D. Fan, O. Shekhah, G. Maurin, M. Eddaoudi and G. Szekely, *Adv. Mater.*, 2024, **36**, 2314206.
69 P. Cai, J. Li, D. Y. Song, N. Zhang, N. X. Zhang and Q. F. An, *J. Membr. Sci.*, 2024, **695**, 122489.
70 S. Li, Y. J. Sun, Z. X. Wang, C. G. Jin, M. J. Yin and Q. F. An, *Small*, 2023, **19**, 2208177.
71 K. Chen, P. Li, H. Y. Zhang, H. X. Sun, X. J. Yang, D. H. Yao, X. J. Pang, X. L. Han and Q. J. Niu, *Sep. Purif. Technol.*, 2020, **251**, 117387.
72 X. Zhang, Y. Zeng, C. Shen, Z. X. Fan, Q. Meng, W. Z. Zhang, G. L. Zhang and C. J. Gao, *ACS Appl. Mater. Interfaces*, 2021, **13**, 48679–48690.
73 Y. T. Lei, L. J. Zhu, J. L. Xu, S. Liu, Z. X. Zeng, X. C. Li and G. Wang, *J. Environ. Chem. Eng.*, 2023, **11**, 111222.
74 Z. H. Li, W. J. Zheng, X. H. Ruan, Y. Dai, X. C. Li, M. Yu, X. B. Jiang, X. M. Wu and G. H. He, *Chem. Eng. J.*, 2024, **495**, 153578.
75 G. Z. Li, Z. H. Si, D. Cai, Z. Wang, P. Y. Qin and T. W. Tan, *Sep. Purif. Technol.*, 2020, **236**, 116263.
76 M. S. Denny Jr. and S. M. Cohen, *Angew. Chem., Int. Ed.*, 2015, **54**, 9029–9032.
77 Y. Jia, K. Y. Chen, P. X. Liu, Y. B. Liu, X. J. Pi, X. C. Zhang and Y. Zhang, *ACS Appl. Mater. Interfaces*, 2024, **16**, 37100–37110.
78 H. Y. Jiao, Y. S. Shi, Y. P. Shi, F. Zhang, K. Lu, Y. T. Zhang, Z. G. Wang and J. Jin, *J. Membr. Sci.*, 2023, **666**, 121146.
79 N. Li, C. Ma, D. D. Li, P. Li, M. Ye, Z. Y. Wang, Z. H. Qiao and C. L. Zhong, *Sep. Purif. Technol.*, 2025, **353**, 128500.
80 F. Y. Li, Y. Xiao, T. S. Chung and S. Kawi, *Macromolecules*, 2012, **45**, 1427–1437.
81 Y. Feng, W. Yan, Z. X. Kang, X. Q. Zou, W. D. Fan, Y. J. Jiang, L. L. Fan, R. M. Wang and D. F. Sun, *Chem. Eng. J.*, 2023, **465**, 142873.
82 A. Kertik, L. H. Wee, M. Pfannmöller, S. Bals, J. A. Martens and I. F. J. Vankelecom, *Energy Environ. Sci.*, 2017, **10**, 2342–2351.
83 X. X. Huang, L. D. Chen, S. Z. Chen, P. C. Su and W. B. Li, *J. Membr. Sci.*, 2023, **685**, 121984.

